Mon. Not. R. astr. Soc. (1989) **240,** 41–61

On the nature of the old nova CP Puppis

D. O'Donoghue and B. Warner *Department of Astronomy, University of Cape Town, Rondebosch 7700, South Africa*

W. Wargau *Department of Mathematics, Applied Mathematics and Astronomy, PO Box 392, Pretoria 0001, South Africa*

A. D. Grauer *Department of Physics and Astronomy, University of Arkansas at Little Rock, Little Rock, Arkansas 72204, USA*

Accepted 1989 February 22. Received 1989 February 17; in original form 1988 December 16

Summary. We report on nearly 48 hr of high speed photometry of the ex-nova CP Pup, obtained at Sutherland or Mount Stromlo, and 23 hr of spectroscopic coverage from Sutherland, during the period 1985–88. Analysis of the photometry and radial velocities derived from the spectroscopy gives a modulation period of 0.06143 d, free from the alias problems inherent in previous work, and identical for both photometry and spectroscopy. This period will not fit the earlier data of Warner and this, together with substantial amplitude variations in the photometric modulation, suggest the presence of more than one photometric periodicity.

Measurements of the radial velocity semi-amplitude give values of ~ 200 km s^{-1} near the emission line centres, decreasing to ~ 120 km s^{-1} in the line wings, but with variations in phase across the line profile. A related V/R effect is seen. There is evidence for repetitive fine structure in the line profiles, but at a level too low to study in detail with the present spectra. If the K velocity of 120 km s^{-1} is representative of the motion of the white dwarf, unreasonable values of the white-dwarf mass and orbital inclination are derived.

No compelling evidence has emerged from the present study to suggest that CP Pup is a magnetic cataclysmic variable, although further study of the behaviour of the photometric modulation may elucidate this question.

1 Introduction

Cataclysmic variables are close binary systems in which a (primary) white dwarf accretes material from a Roche-lobe-filling secondary star. Several sub-classes are recognized (see Warner 1976; Robinson 1976; Cordova & Mason 1983 for reviews), the most obvious classification criterion being the way in which the gas accretes on to the white dwarf. This in turn depends on the strength of the white dwarf's magnetic field: if the field is weak, the material

forms an accretion disc (Pringle 1981) and ultimately falls on to the white-dwarf surface via a boundary layer at the inner edge of the disc. On the other hand, if the field is strong ($B \sim 10^7$ G), no disc is expected to form: instead, the material is channelled by the magnetic field on to the white dwarf. Such systems are known as 'polars' or AM Her systems [see Liebert & Stockman (1985) for a review]. Another important discriminant in classification is the long-term variability in the system luminosity: for example, classical novae are recognized by their dramatic eruption; 'nova-like' variables (excluding stars such as PU Vul or P Cyg for which this term is inappropriate) are believed to be the same kind of object except that they lack a recorded nova eruption. Dwarf novae, on the other hand, exhibit much more frequent outbursts (repeating every few weeks or months) with, as the name implies, considerably lower amplitude.

Observationally, there is little overlap between many of the subclasses. For example, until recently, few classical novae were known to show dwarf nova outbursts and none were known with an orbital period below the period gap (Robinson 1983) or to be strongly magnetic [see Livio & Shara (1987) for a discussion]. Elaborations on the basic model for cataclysmic variables in terms of differing magnetic field strength or mass transfer rate have been proposed to explain the various subclasses, but these are far from secure. As a result, examples of cataclysmic variables which are members of more than one subclass are of special interest. As will become clear below, V1500 Cygni (Nova Cygni 1975) and CP Puppis (Nova Puppis 1942) are two such examples.

Warner (1985) has drawn attention to the similarity of CP Pup and V1500 Cyg: in eruption, they were both very fast novae of very large range relative to their pre-nova brightness. However, in each case, the brightness of the pre-nova was much fainter than the (present) brightness of the remnant, both of which appear to be at the end of their decline from eruption.

Spectroscopic variations with a period of 3.3 hr were found in V1500 Cyg at the time of its eruption (Campbell 1976; Hutchings & McCall 1977); the system also exhibits photometric variations with a similar period whose precise value varied erratically at the time of the eruption but stabilized after two years (Kruszewski, Semeniuk & Duerbeck 1983; Lanning & Semeniuk 1981; Patterson 1978, 1979). The resemblance between CP Pup and V1500 Cyg was therefore further strengthened by the discovery in CP Pup (Warner 1985) of recurrent photometric humps with a period of ~ 1.5 hr. Curiously, radial velocity variations with a period close, but not quite equal, to the period (or its alias) found by Warner (1985) were reported by Bianchini, Friedjung & Sabbadin (hereafter BFS) (1985a,b,c). The ~ 1.5-hr period in CP Pup and the 3.3-hr period in V1500 Cyg have been interpreted (e.g. Warner 1985) as being equal, or close to, the orbital period of the system. If correct, CP Pup would become the first ex-nova with an orbital period below the 'period gap'.

V1500 Cyg has recently been demonstrated to be a strongly magnetic system by the discovrery of variable optical circular polarization (Stockman, Schmidt & Lamb 1988). Remarkably, the period of the polarization variations is 1.8 per cent shorter than the stabilized photometric period (Kaluzny & Semeniuk 1987). This has been interpreted by Stockman *et al.* (1988) as being due to a slight asynchronism between the region emitting the polarized light (assumed to be an accretion column 'anchored' to the strongly magnetic primary white dwarf) and the secondary star (whose reflection effect is presumed to be the source of the photometric variations). In AM Her systems, the white dwarf is phase-locked to the secondary star by the magnetic field of the white dwarf so that the slight asynchronism in V1500 Cyg has been interpreted by Stockman *et al.* (1988) as a consequence of the nova outburst in what was previously a phase-locked binary. The erratic behaviour of the photometric period at the time of the eruption provides support for this hypothesis.

As a consequence of the discovery of the magnetic nature of V1500 Cyg, interest in CP Pup is now acute: in spite of the lack of detection of circular polarization in CP Pup (Cropper 1986;

Stockman *et al.* 1988), its similarity to V1500 Cyg suggests that it may also be a magnetic system, possibly asynchronized. The periods reported in the studies of Warner (1985) and BFS (1985a,b,c) suffer from aliasing difficulties and, to add to the confusion, a different spectroscopic period has recently been claimed by Duerbeck, Seitter & Duemmler (1987) (hereafter DSD). This paper presents new spectroscopic data which will settle the uncertainties concerning the spectroscopic period. In addition, new photometric data are reported, the most recent of which (1988 March) were obtained contemporaneously at SAAO and Mount Stromlo observatories as a secondary observing programme in the Extended Coverage Project (a campaign to obtain 24-hr coverage of rapidly variable stars using a global network of observers in both hemispheres). These efforts have resolved the aliasing problem in the photometric period arising from the earlier studies but, as a result of instabilities in this period, its interpretation is still not clear.

2 Observations

2.1 PHOTOMETRY

The new data comprised high-speed photometric observations obtained at the Sutherland observing station of the South African Astronomical Observatory using the 0.75-m and 1.0-m reflectors during 1985 April, 1986 January, 1986 April and 1988 March and at Mount Stromlo Observatory using the 1.9-m reflector during 1988 March. All observations were made in 'white light' using two-star photometers (Nather & Warner 1971). With the exception of run S3498 in 1985 April, which used an RCA 31034A photomultiplier tube with an extended red response, all the data were collected with photomultiplier tubes whose blue spectral response corresponds to an effective wavelength close to that of a Johnson *B*-filter. An observing log appears in Table 1. Note that the Mount Stromlo data (runs A24, A25 and A27) were taken contemporaneously with some of the SAAO data. Each run was reduced by

Table 1. Photometric observing log.

Run	Start date & time (UT)						HJD (2440000+)	Tel. (m)	S (s)	Length (hr)	Mean B mag
S3498	9	4	85	18	1	28	6165.25264	1.0	4.0	5.1	
S3753	9	1	86	22	48	55	6440.45361	1.0	5.0	3.0	15.0
S3757	11	1	86	22	11	31	6442.42769	1.0	5.0	3.7	15.0
S3761	12	1	86	21	41	47	6443.40707	1.0	5.0	3.5	15.0
S3763	13	1	86	20	30	32	6444.35761	1.0	5.0	5.3	15.0
S3766	16	1	86	0	26	40	6446.52165	0.75	5.0	1.7	15.2
S3768	17	1	86	0	31	0	6447.52468	0.75	5.0	1.5	15.8
S3773	20	1	86	0	5	0	6450.50668	0.75	5.0	2.1	15.1
S3809	11	4	86	19	30	35	6532.31443	0.75	5.0	1.0	15.1
S3812	12	4	86	18	17	35	6533.26368	0.75	5.0	1.7	15.1
S4228	14	3	88	19	27	20	7235.31339	1.0	10.0	1.6	15.1
S4231	15	3	88	19	22	0	7236.30965	1.0	10.0	1.6	15.1
S4233	16	3	88	18	9	10	7237.25904	1.0	10.0	3.0	15.2
S4236	17	3	88	18	3	20	7238.25495	1.0	10.0	2.1	15.1
S4239	18	3	88	18	16	0	7239.26371	1.0	10.0	.8	15.1
S4240	18	3	88	20	7	37	7239.34122	1.0	10.0	.8	15.1
A24	19	3	88	12	0	0	7240.00257	1.9*	5.0	1.6	
A25	20	3	88	10	12	30	7240.92788	1.9*	5.0	2.4	
S4244	20	3	88	17	56	0	7241.24975	1.0	10.0	2.5	15.2
A27	21	3	88	12	25	0	7242.01986	1.9*	10.0	1.8	
S4248	21	3	88	19	15	0	7242.30457	1.0	10.0	.8	15.2

* denotes at Mt. Stromlo Observatory.

subtracting the sky background, linearly interpolating over gaps in the data and correcting for extinction using a mean extinction coefficient. The last column of Table 1 provides the equivalent mean *B* magnitude for each run.

2.2 SPECTROSCOPY

All the spectra were obtained with the reticon detector (Glass 1982) attached to the image tube spectrograph on the 1.9-m reflector at Sutherland. The spectral region from 3600 to 5400 Å was covered at a resolution of ~ 3 Å (FWHM) using a dispersion of 75 Å mm^{-1}. In order to resolve variability on the 1.5-hr period, short exposures were used, usually less than 500 s but occasionally as long as 720 s. The object was detected using one array of the reticon and sky subtraction was achieved by observing a nearby sky region with the other array; with the exception of the observation on 1988 March 17, the object was swapped between arrays regularly, usually after every second exposure. In order to minimize possible systematic or sudden wavelength shifts, and thereby obtain the most accurate radial velocities, only one array of the reticon was used to detect the object spectrum on 1988 March 17. A Cu/Ar arc spectrum was observed at least every half hour. Flat-field calibration spectra were obtained at the beginning and end of each night and a nearby spectrophotometric standard star was observed just before or after CP Pup. Observing details for the 90 spectra obtained in 1985 April and 52 spectra obtained in 1988 March are listed in Table 2.

Table 2. Spectroscopic observing log.

Date	Start (UT)	End (UT)	Exposure Time (s)	No. of Spectra
9 4 1985	19:04	23:01	480	24
10 4 1985	18:07	21:54	720,480	2,20
11 4 1985	18:04	22:46	480	28
13 4 1985	19:25	22:05	420	14
15 4 1985	18:17	18:40	480	2
15 3 1988	20:35	23:03	600	12
16 3 1988	19:03	21:41	480	16
17 3 1988	18:28	21:56	450	24

The spectra were reduced using standard techniques: pixel-to-pixel variations in the reticon arrays were removed by dividing by the flat-field spectrum. The wavelength calibration was defined by fitting a fifth-order polynomial to the comparison arc spectra; the mean residual about this fit and the shift in the wavelength calibration from arc to arc were found to be less than 0.2 Å. This calibration was used to resample the arrays at equal wavelength intervals. The sky spectra were then subtracted from the star spectra and a flux calibration applied derived from observations of the flux standard stars.

2.3 *EXOSAT* OBSERVATIONS

At our request, Dr I. McHardy made an observation of CP Pup on 1985 April 9/10 from 18.55–00.56 UT using the *EXOSAT* satellite, simultaneously with photometry (run S3498) and spectroscopy obtained on that date. CP Pup was detected as a weak source in the 2–6 keV range using the medium-energy detector array (~ $10^{11.6}$ erg cm^{-2} s^{-1}) and marginally detected with the low-energy imaging telescope, consistent with a previous X-ray observation (Becker & Marshall 1981). There is evidence in the X-ray light curve that the source is variable but no correlation between the optical light curve and the apparent X-ray variability could be found.

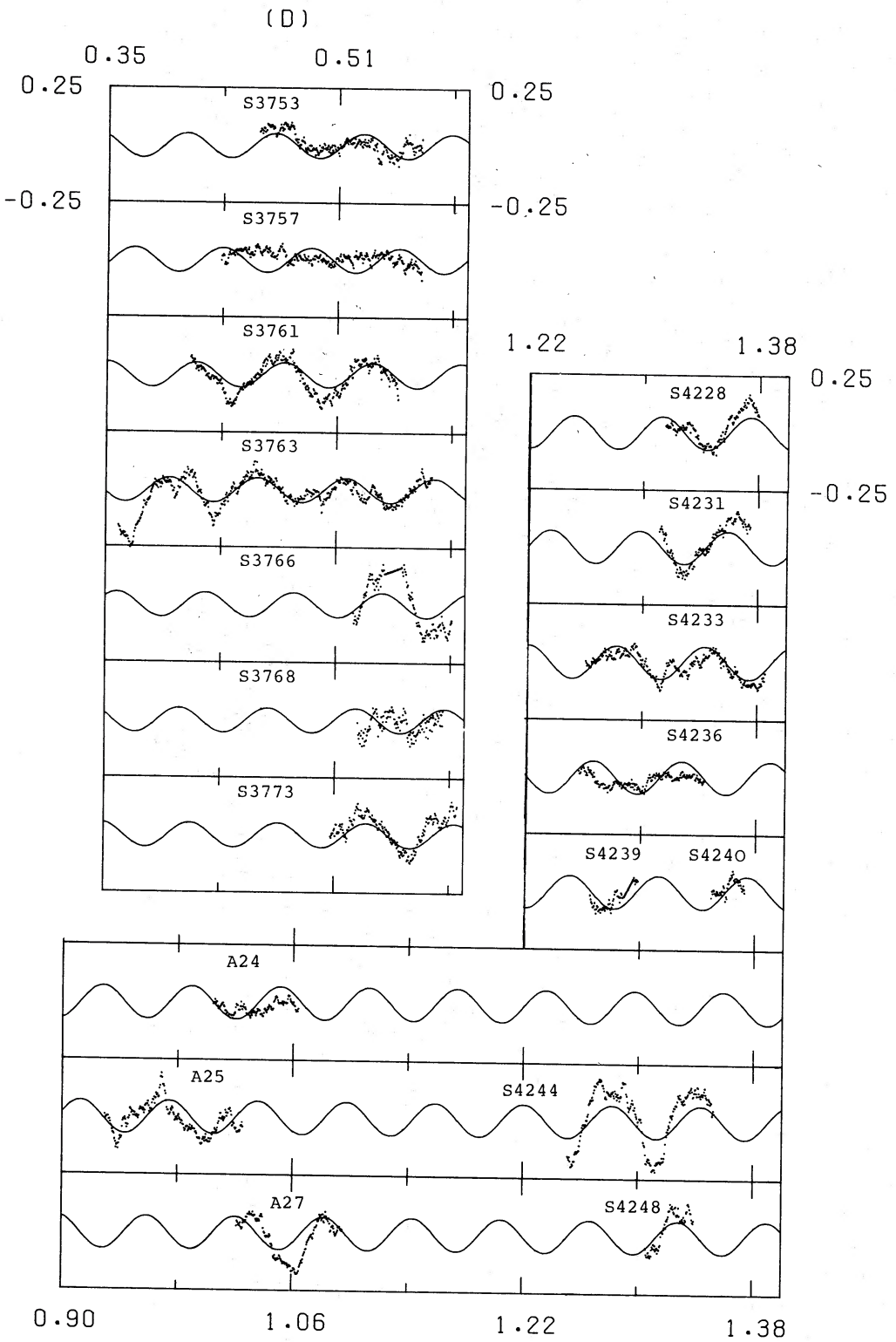

Figure 1. A plot of the photometric data listed in Table 1. The ordinate is in units of the mean brightness during the run, the corresonding *B* magnitude of which appears in Table 1. The original data were summed into 40-s bins to yield the plotted points. Run numbers are indicated above the corresponding light curve. The abscissa is fractional Heliocentric Julian Date. The solid lines represent the best-fitting sinusoids of Table 3.

3 Photometric results

The photometry listed in Table 1 is displayed in Fig. 1. As found by Warner (1985), the light curve shows a modulation with a period of ~1.5 hr together with flickering on time-scales as short as 100 s. A power spectrum of each run revealed no rapid oscillations in the frequency range 10–50 mHz with amplitudes exceeding 0.002 mag. As noted by Warner (1985), the ~1.5-hr modulation resembles the 3.3-hr variations of V1500 Cyg and shows a variety of pulse shapes with significant changes on a short time-scale (*cf.* runs A25 and S4244 which are separated by less than 8 hr). The search for and detection of polarization in V1500 Cyg was prompted by the similarity of its light curve (sharp rises and falls) to those of the AM Her stars (Kaluzny & Semeniuk 1987). In this connection, it is of interest to note the rapid variations in CP Pup in run A25 and the resemblance between run S4244 and the light curve of AM Her shown in Szkody & Brownlee (1977). The most striking feature of the new data when compared with the earlier (1985 February) observations of Warner (1985) (his fig. 1) is that the ~1.5-hr modulation shows a larger range in amplitude, reaching as high as 40 per cent (peak-to-peak) of the mean brightness of the star (e.g. runs A25 and S4244) but also frequently showing little or no evidence for variability on this time-scale (e.g. runs S3753, S3757, S4236 and A24). An inspection of runs S4228–S4248 in Fig. 1 (in which data were obtained on each of eight consecutive days) shows that the amplitude of the photometric modulation varies smoothly from day to day, giving a strong impression of the beating of two periods on a time-scale of about a week. A qualitatively similar kind of variation occurs in S3753–S3773 but, in this data set, the amplitude can change on a shorter time-scale (see run S3763). There is little evidence of amplitude variation in the data reported by Warner (1985). We will discuss the possible presence of more than one photometric period in more detail after the aliasing problems arising in the study of Warner (1985) have been resolved.

The most viable technique for determining the precise period of the ~1.5-hr modulation is Fourier analysis: the changes in pulse shape preclude the use of other techniques which do not assume a sinusoidal variation (e.g. phase dispersion minimization techniques). Fourier amplitude spectra were calculated for two subsets of the data in Table 1: runs S3761–S3773 and runs S4228–S4248 (note that the ~1.5-hr modulation is essentially absent in runs S3753 and S3757 so these data were excluded from the Fourier analysis of the 1986 January data set). The data of Warner (1985) (runs S3484–S3489) were also available and re-analysed. The Fourier amplitude spectra of these data sets are shown in Fig. 2 and the corresponding spectral windows (Deeming 1975) are shown alongside. Note that the 1 cycle d^{-1} in the spectral window of S4228–S4248 is quite small due to the combination of the South African and Australian data and that the high-frequency aliases in the amplitude spectrum of this data set are suppressed. It is clear that highest peak in the amplitude spectrum of S4228–S4248 is the correct period as its 3 cycle d^{-1} alias can be discounted from consideration of the other amplitude spectra. This peak is also the highest in the amplitude spectrum of S3761–S3773 and is approximately equal to the shorter of the possible periods found by Warner (1985). The amplitude and phase of this period were found for each data set by fitting a sinusoid to the data by least squares. The resulting parameters are listed in Table 3 and the best-fitting sinusoids are shown as solid lines in Fig. 1.

A discussion of the errors on the values listed in Table 3 is warranted: the formal error on the time of maximum obtained from fitting by least squares a sinusoid of the appropriate period to the data is about 0.0003 d and, due to the substantial intrinsic 'jitter' (see Fig. 1) of the time of maximum of each pulse [up to 0.15 cycles (Warner 1985)], this estimate is likely to be too small. Owing to the phase 'jitter' and variations in amplitude, estimating the error on the period is not straightforward. We believe that the periods derived from the new photometric

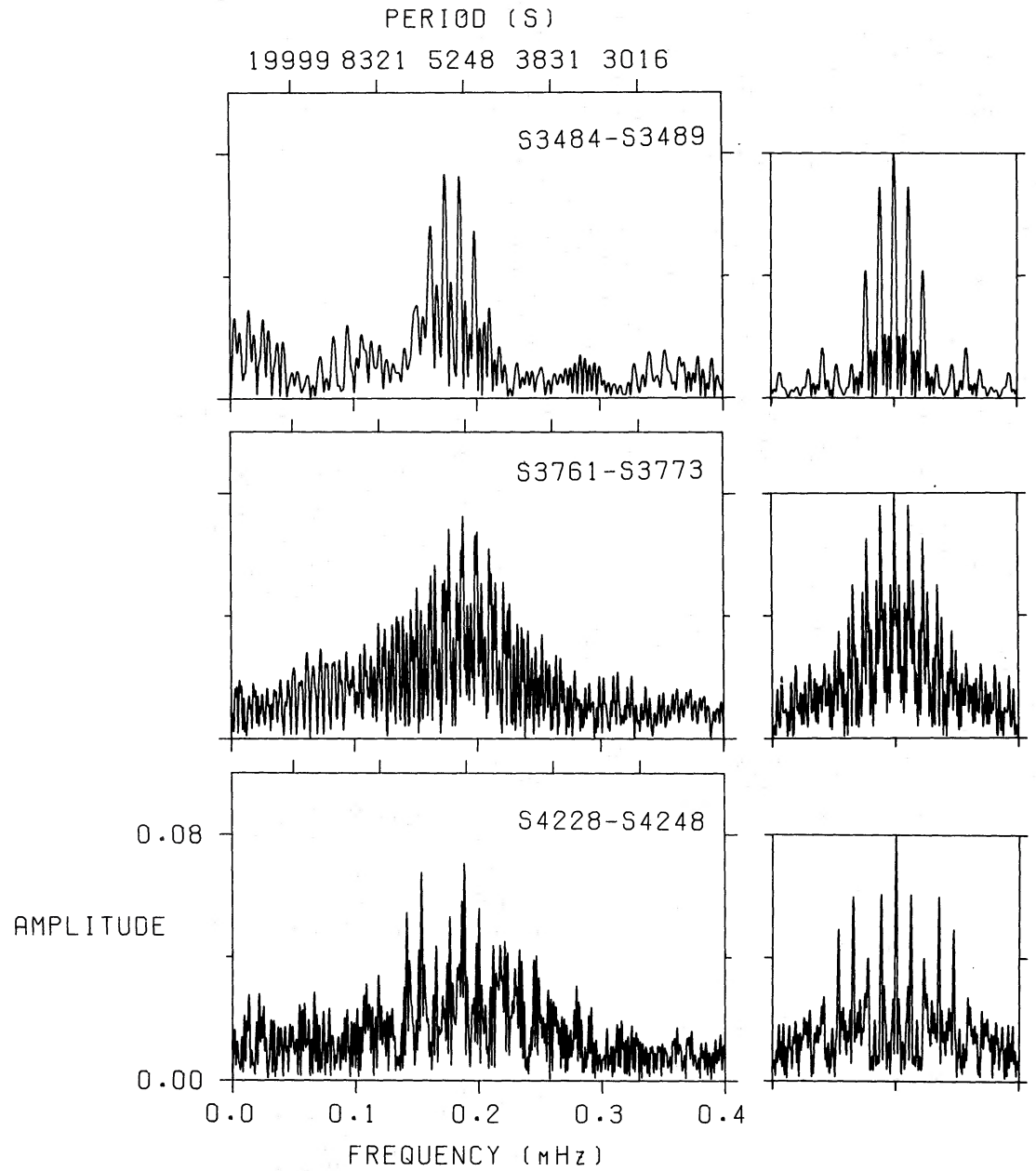

Figure 2. Fourier amplitude spectra of the photometry in Table 1 and of Warner (1985). The ordinate units are the same as for Fig. 1. The spectral window for the data sampling is shown alongside.

data sets (S3761–S3773 and S4228–S4248) are consistent with each other and consistent with the spectroscopic period to be discussed below. However, the period from S3484–S3489 is too long to be consistent with any of these periods. We checked this conclusion by fitting a sinusoid with a period of 0.06154 d (as found for S4228–S4248) to S3484–S3489 with the

Table 3. Fourier analysis of photometric modulations.

Data set	Period (days)	Mean Semi-Amplitude	Time of Maximum Hel. Jul. Date
S3489-S3489	0.06198	0.073	6112.3446
S3761-S3773	0.06138	0.074	6443.4119
S4228-S4248	0.06154	0.071	7235.3119

result that its peaks came systematically 'late' in S3484 and S3486 and 'early' in S3487 and S3489 and generally gave a very poor fit to the data (as is expected from the 'wrong' period).

We now investigate whether the phase 'jitter' and period inconsistencies mentioned above result from modelling the data with a single sinusoid with constant amplitude and phase. As we have seen, there is evidence for 'beating' of two or more periods in the data. We therefore subracted the best-fitting sinusoids shown in Fig. 1 from the data sets S4228–S4248 and S3753–S3773 and calculated the Fourier amplitude spectrum of the residuals of each data set. As expected, there was significant power left in the resulting amplitude spectra. However, there were no periods or their aliases in common between the two data sets. We note that the detection of other possible periods requires continuous coverage of at least 1.5 'beat cycles' (Loumos & Deeming 1978) (or, presumably, many beat cycles if the data are not continuous) and conclude that the available data are too limited to determine whether there is more than one stable period near ~ 1.5 hr.

4 Spectroscopic results

4.1 MEAN SPECTRA

Fig. 3 shows the sum of all the spectra obtained during 1988 March and 1985 April, summed separately. Apart from the slight difference in strength of He II λ4686 Å, there are no significant differences between these spectra. Although the signal-to-noise ratio of the individual exposures is obviously much worse, and therefore only strong variations would be discernible, inspection revealed no such short-term variability in the spectral features, contrary to the claims of BFS (1985b). The spectrum shows emission lines superimposed on a blue

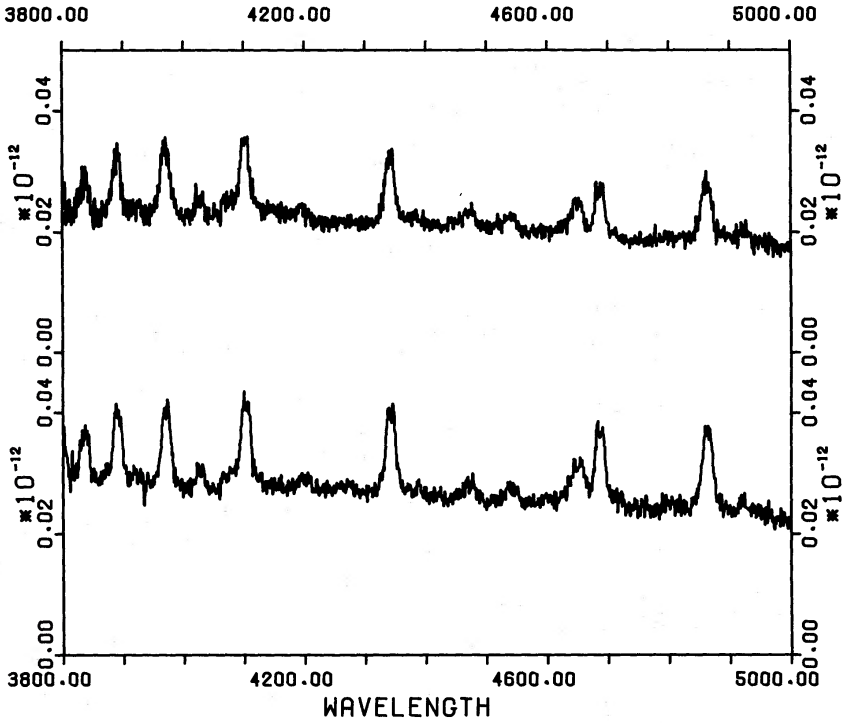

Figure 3. The mean spectrum of CP Pup during 1985 April (lower) and 1988 March (upper), summed separately. The units of the abscissa are Å and those of the ordinate are erg s^{-1} cm^{-2} $Å^{-1}$. The ordinate scale is intended as a rough indication only as the data were acquired with a slit; the origin for the upper curve is indicated half way up the panel.

continuum. The Balmer lines are resolved up to H10 and show a flat decrement characteristic of optically thick lines. There is evidence that the lines are doubled in the 1985 April spectrum; the modest signal-to-noise and resolution of the spectrum prevented more than a rough estimate of the separation of the components: 550 km s^{-1}. The remaining features are high excitation lines typical of both ex-novae and AM Her systems: He II (λ4686 Å especially prominent, $\lambda\lambda$4545 and 4200 Å), He I ($\lambda\lambda$5015, 4921, 4471 and 4026 Å), the C III–N III blend and C II λ4267 Å. There is evidence for He I λ4388 Å in the red wing of Hγ and a broad feature in the blue wing of Hδ. This feature is visible in the spectrum of V1500 Cyg but was not remarked upon by Kaluzny & Chlebowski (1988). Its central wavelength was defined by fitting a Gaussian profile and was found to be 4072 Å; it is also seen in LX Ser (Young, Schneider & Schectman 1981) and may be ascribed to the O II blend in the $\lambda\lambda$4070, 4072 and 4076 Å region. Over all, the spectrum of CP Pup is virtually identical to that of V1500 Cyg (Kaluzny & Chlebowski 1988).

Table 4. FWHM and equivalent widths.

	FWHM (Å)		Equivalent Width (Å)	
	1985 April	1988 March	1985 April	1988 March
	(±2Å)		(±2Å)	
Hβ	22	20	16	13
Hγ	20	19	14	13
Hδ	20	20	14	14
Hε	17	21	11	15
H8	16	16	8	9
H9	17	17	7	7
H10	13	10	3	3
	(±4Å)		(±2Å)	
λ4471	31	36	5	6
λ4026	18	16	4	3
λ4686	17	20	11	13
λ4541	26	33	4	5
λ4200	25	23	3	2

Measurements of the full widths at half maximum (FWHM) and equivalent widths have been made for all the lines in Fig. 3 by fitting Gaussian profiles. The results are listed in Table 4. The hydrogen lines are moderately broad (FWHM ~ 1500 km s^{-1}) and decrease in width up the series. This behaviour is expected if the broadening is due to Doppler rotation in an accretion disc. The uncertainty of measurement precludes a rigorous, quantitative test of this hypothesis. Some of the helium lines are much broader than the hydrogen lines (He I λ4471, He II $\lambda\lambda$4541, 4200 Å). Note that λ4471 and λ4541 appear asymmetric as though there is another unresolved line in the blue wing, especially in the 1985 April sum spectrum. Anomalously blueshifted γ-velocities were also found for λ4541 and λ4200 in the analysis described in the next section and we note that there are prominent N III lines in their wings. We conclude that the anomalous breadths of some of the lines are probably due to blending with unresolved, weaker lines.

4.2 SPECTROSCOPIC PERIOD

In order to resolve the uncertainties concerning the spectroscopic period (BFS 1985a,b,c; DSD), a search for periodic radial velocity variations was carried out. The method used in the first instance was the cross-correlation method of Tonry & Davis (1979) in which each spectrum is resampled into equal log wavelength (or velocity) bins and cross-correlated with a

template spectrum, similarly resampled. The shift required to bring the two spectra into register then yielded the relative radial velocity. In the present application, the sum of all the spectra obtained in 1988 March was used as the template which, as a result of its similarity to the sum of all the 1985 April spectra (Fig. 3), was suitable for cross-correlating with the 1985 spectra as well. The resulting radial velocities were placed on an absolute scale by measuring the velocity of the template using the technique described in Section 3.3. A clear variation with a period of ~0.06 d is apparent in the results, which are plotted in Fig. 4 (lower) and listed in Table 5a. Fourier amplitude spectra of the two data sets are shown in Fig. 4 (upper) (there were no significant peaks in the 0.5–1.0 mHz region); the highest peak in each is flanked by a

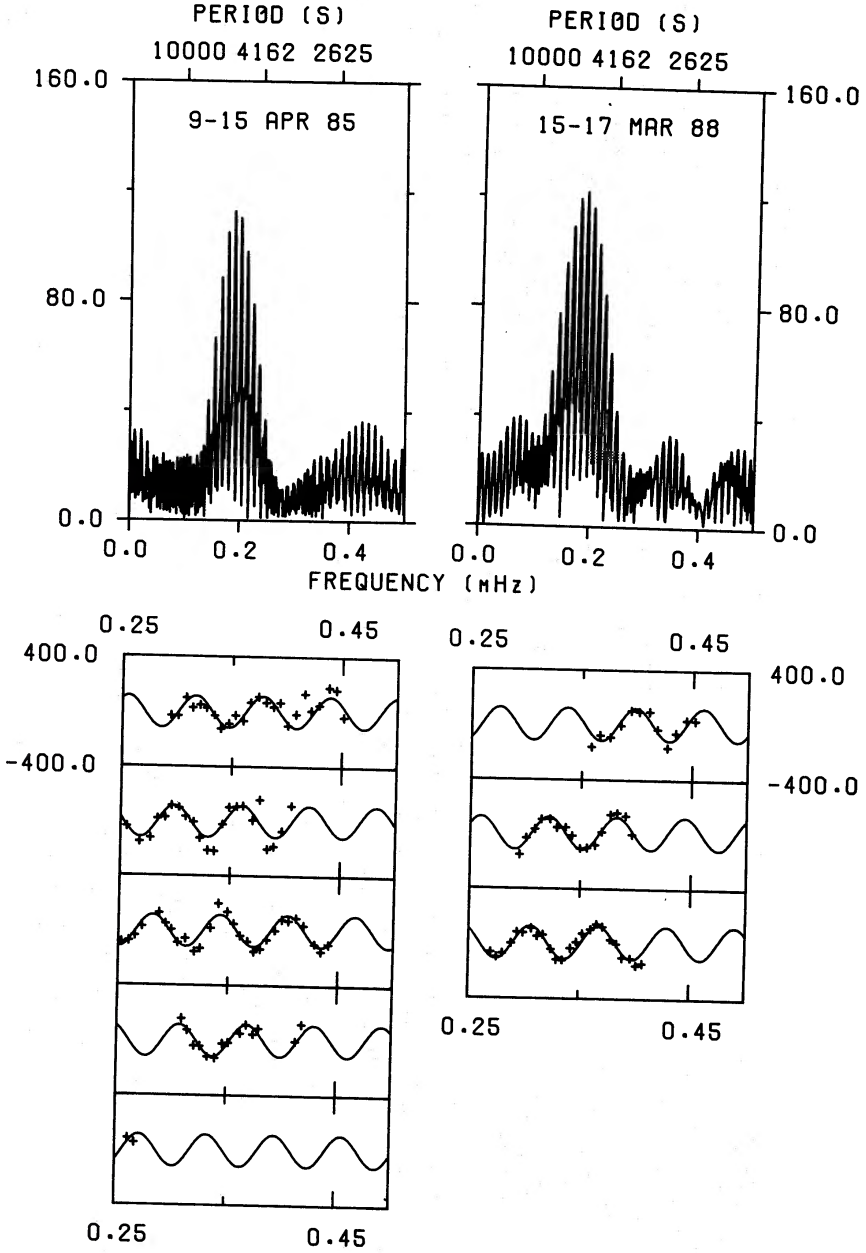

Figure 4. Radial velocities of the individual spectra listed in Table 2 (lower panels) and their Fourier amplitude spectra (upper panels). The abscissae of the lower panels are in days. The ordinate of all panels is in km s^{-1}. The solid lines in the lower panels are the best-fitting sinusoids with periods given by the highest peaks in the upper panels.

Table 5. (a) Heliocentric velocities of individual spectra.

1985 April				1988 March	
$JD_\odot$	(km s^{-1})	$JD_\odot$	(km s^{-1})	$JD_\odot$	(km s^{-1})
6165.29736	6	6167.30127	40	7236.36230	-155
6165.30371	4	6167.30713	-54	7236.37012	-71
6165.31104	135	6167.31396	-22	7236.37939	-84
6165.31689	64	6167.32227	-118	7236.38867	1
6165.32373	85	6167.32764	-94	7236.39795	111
6165.32959	63	6167.33691	54	7236.40527	104
6165.33691	7	6167.34375	233	7236.41455	104
6165.34277	-88	6167.35205	172	7236.42188	-25
6165.35010	-51	6167.35791	86	7236.43115	-157
6165.35596	9	6167.36377	-1	7236.43848	-52
6165.36328	-30	6167.37061	-42	7236.44824	41
6165.36963	104	6167.37646	-115	7236.45605	38
6165.37695	147	6167.38232	-97	7237.29883	-149
6165.38379	104	6167.38818	-29	7237.30469	-27
6165.39063	74	6167.39551	38	7237.31250	38
6165.39648	104	6167.40186	119	7237.31836	108
6165.40381	-63	6167.40771	109	7237.32617	111
6165.41113	21	6167.41455	131	7237.33252	50
6165.41895	171	6167.42139	76	7237.34033	52
6165.42480	48	6167.43164	-59	7237.34619	-8
6165.43213	89	6167.43750	-110	7237.35352	-102
6165.44092	218	6167.44434	-59	7237.35986	-97
6165.44775	201	6169.31201	193	7237.36719	-76
6165.45459	2	6169.31738	108	7237.37305	20
6166.25879	-5	6169.32373	-4	7237.38086	147
6166.27051	-117	6169.32910	-7	7237.38672	161
6166.28027	-88	6169.33594	-84	7237.39453	138
6166.28662	52	6169.34277	-91	7237.40039	2
6166.29346	63	6169.34961	12	7238.27393	-63
6166.29932	148	6169.35498	18	7238.27930	-99
6166.30615	133	6169.36572	88	7238.28467	-73
6166.31201	69	6169.37109	150	7238.29248	1
6166.31934	28	6169.37744	80	7238.29785	82
6166.32520	-88	6169.38232	122	7238.30322	80
6166.33252	-178	6169.41602	31	7238.31055	111
6166.33838	-183	6169.42139	155	7238.31592	52
6166.34570	12	6171.26465	120	7238.32129	64
6166.35156	138	6171.27051	89	7238.32861	-40
6166.35840	142			7238.33350	-115
6166.36426	147			7238.33887	-119
6166.37305	45			7238.34619	-32
6166.37939	194			7238.35156	12
6166.38672	-166			7238.35693	75
6166.39258	-147			7238.36426	106
6166.39990	-35			7238.36963	143
6166.40820	152			7238.37500	127
6167.25586	-52			7238.38232	31
6167.26270	-41			7238.38770	2
6167.26807	-3			7238.39307	-98
6167.27441	64			7238.40039	-103
6167.29004	162			7238.40576	-155
6167.29590	85			7238.41113	-139

symmetrical pattern of 1 cycle d^{-1} aliases and is the same for each data set, indicating that it is the correct alias. The resulting periods were refined by fitting a sinusoid of variable amplitude, period and phase to the data by non-linear least squares. These fits are plotted in Fig. 4 (lower) and their parameters are listed in Table 5b. The standard deviation of the residuals about the fit was 60 km s^{-1} for the 1985 April data and 40 km s^{-1} for the 1988 March data.

The periods derived from the new data are in satisfactory agreement with each other and with the period reported by DSD (also in Table 5b) but are in poor agreement with either of the periods reported by BFS (1985a,b or c). Plots of the velocities published by DSD and

Table 5. (b) Fourier analysis of radial velocities.

Data set	Period (days)	K ($km\ s^{-1}$)	Superior Conjunction (HJD)	γ ($km\ s^{-1}$)
1985 April	0.06141 ±3	117 ±9	6165.3342 ±11	34 ±10
1988 March	0.06148 ±5	121 ±7	7236.4183 ±11	8 ±10
Duerbeck *et al.*	0.06143 ±3	92 ±18		29 ±12
Bianchini *et al.* (1985a,b)	0.06115			

(especially) BFS (1985b, c) showed that these were much noisier than the data presented here. This results in the larger error on the velocity semi-amplitude quoted by DSD; the comparable uncertainty in their period determination is a consequence of the longer baseline over which their data were obtained. Attempts to bridge the one-year gap between the 1985 April data and those of BFS (1985a, b or c) were defeated by a multiplicity of aliases (more than a dozen) in the Fourier spectrum of the combined data set. Therefore, solutions 2 and 3 published by DSD, resulting from an attempt to bridge a 2-yr gap with noiser data, should be disregarded; it is unsafe to extrapolate more than a month beyond the data sets presented here or by DSD. Unfortunately, this excludes bridging the three-month gap between the infrared data of Szkody & Feinswog (1988) and the 1988 March spectroscopy.

As mentioned above, if the spectroscopic period is due to orbital motion, CP Pup would become the first ex-nova with an orbital period shorter than the period gap (Robinson 1983); it is therefore worth considering briefly the possibility that this period is not the orbital period. For example, V1668 Cyg (Nova Cyg 1978) exhibited a 10.54-hr period shortly after eruption (Campolonghi *et al.* 1980) while a tentative period of 1.7 hr was reported by Piccioni *et al.* (1984). Two periods (0.116 and 0.615 d) have also been reported for the nova-like variable V795 Her (PG1711+336) (Mironov, Moshkalev & Shugarov 1983; Thorstensen 1986; Shafter *et al.* 1987). In contrast, there is no evidence in Fig. 4 for a longer spectroscopic period in CP Pup. There is also no sign of the spectrum of the secondary in the red spectrum published by DSD. Moreover, Szkody & Feinswog (1988) have detected a modulation in the infrared at approximately half the spectroscopic period. Such a modulation is typical of the ellipsoidal variations of the Roche-lobe-filling secondary in cataclysmic variables [see Szkody & Feinswog (1988) and references therein] and is strong supporting evidence that the spectroscopic period is the orbital period of CP Pup. As a result we have folded all the spectra into ten phase bins for each season separately, using the ephemerides in Table 5b, and performed all subsequent analyses on these two sets of phased spectra. These binned spectra show line profile variations with orbital phase and are displayed in Fig. 5.

4.3 ORBITAL VARIATIONS

The orbital variations of the emission lines in cataclysmic variables are poorly understood. The commonly made assumption in non-magnetic systems is that the lines are formed in the accretion disc surrounding the primary white dwarf and that these lines can be expected to share the motion of the white dwarf. A recognized complication arises from the possible

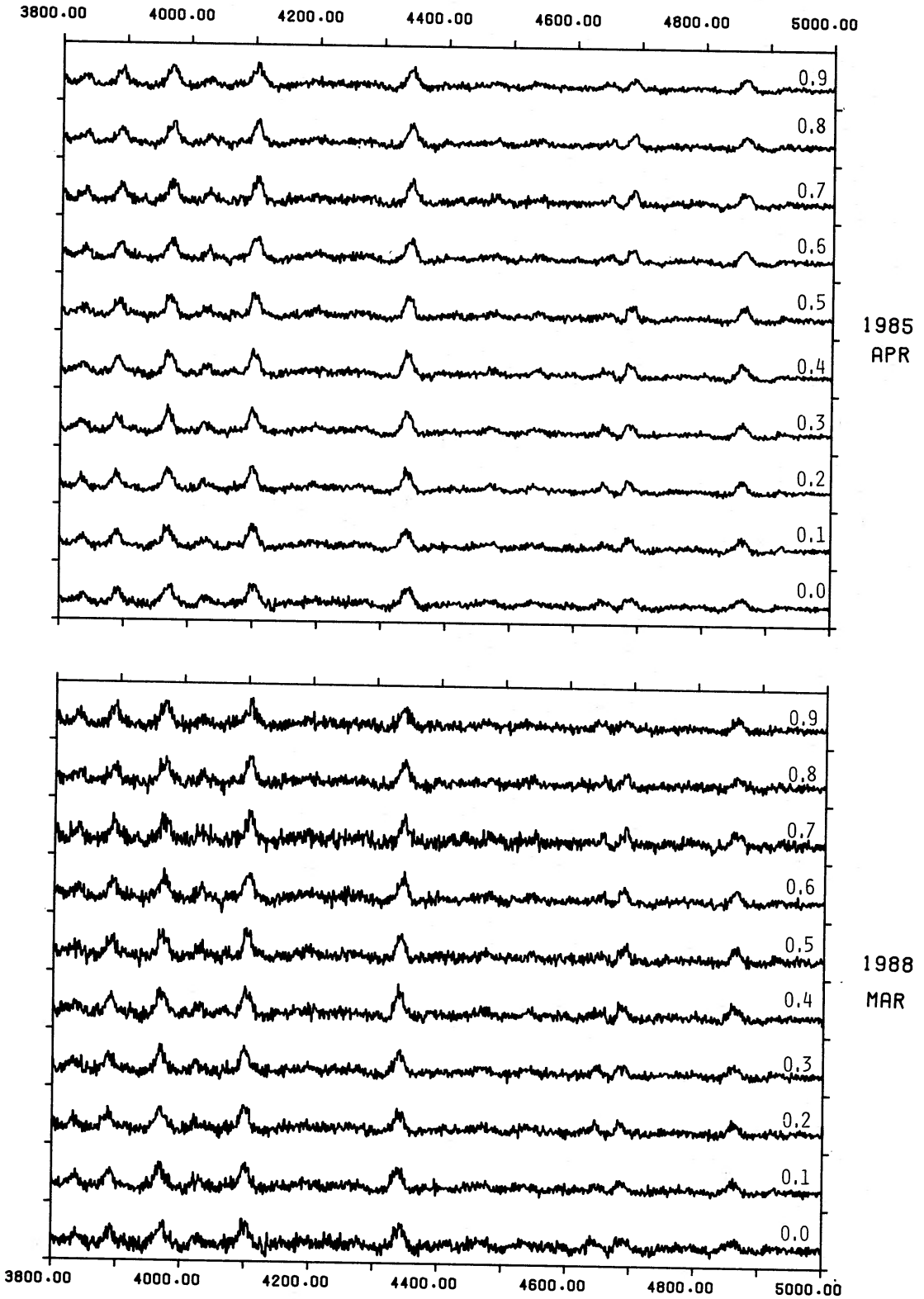

Figure 5. Spectra folded into ten orbital phase bins for each season separately using the ephemerides of Table 5b. Orbital phase is indicated above the corresponding spectrum. Each spectrum was normalized by the total number of counts in the spectrum and the slope of the continuum was removed. The ordinate scale is therefore arbitrary but the same for all spectra in the panel. Abscissa units are Å. The slight depressions surrounding the Balmer emission lines are an artefact of the technique used to remove the continuum slope and are not very broad absorption features.

distortion of the line profiles by a narrow component in the line core (often referred to as an 's-wave') due to a region of enhanced emission located at the bright spot. However, in cases where the position in orbit of the component stars is available from other information (either through detection of the absorption spectrum of the secondary as in the dwarf nova V426 Oph (Hessman 1988), or through eclipses as in the possible low-field polar V2051 Oph (Warner & O'Donoghue 1987; Watts *et al.* 1986), differences between the γ crossing of the radial velocity curve of the emission line source and the conjunction of the component stars can be as large as 50°, even when the extreme wings of the emission lines are used for measurement. In addition, the orbital variations of narrow components in the line cores in many systems are inconsistent with the behaviour expected from a region of enhanced emission located at the bright spot. For instance, in the nova-like variables UX UMa (Schlegel, Honeycutt & Kaitchuck 1983) and RW Tri (Kaitchuck, Honeycutt & Schlegel 1983), regions of enhanced emission along the line of centres at the edge of the disc between the two stars were proposed to explain their observations. More spectacularly, Shafter, Szkody & Thorstensen (1986) were forced to suggest a region of enhanced emission on the side of the disc directly opposite the bright spot to explain the behaviour of the narrow component in the emission line core of the dwarf nova SW UMa.

In order to determine whether the emission lines in CP Pup are subject to such anomalies, we employed the double Gaussian mask technique devised by Schneider & Young (1980) and elaborated by Shafter (e.g. Shafter 1983; Shafter *et al.* 1986) to map out the orbital variations of different parts of the line profiles. In this technique, two Gaussians of specified σ are positioned in the wings of an emission line at a distance a from the rest wavelength. Holding σ and a constant, the shift is determined for which the convolution of each Gaussian with the line profile yields equal fluxes. This shift is then a measure of the radial velocity of the spectrum. As discussed by Shafter (1983), obtaining a radial velocity curve for various values of the parameter a shows how its amplitude is affected by which part of the line profile is selected for measurement. We used this technique on both the individual Balmer lines and He II λ4686 Å with $a = 350$ km s^{-1} and a large σ of 500 km s^{-1} taking in most of the line profile. Having determined that there were no gross differences in behaviour among the lines of the same species, we also used it on all the unblended lines of the species simultaneously in order to maximize the signal to noise. In this case, the method has been generalized so that a pair of Gaussians is used for each line and it is necessary to determine the *velocity* shift which must be applied to all the pairs to yield equal counts in the sum of the convolutions of the Gaussians with the blue and red wings of all the lines. The Balmer lines were found to be sufficiently strong so that rather narrow Gaussians with $\sigma = 175$ km s^{-1} could be used, with values of a from 175 km s^{-1} (sampling the line core) to 1050 km s^{-1} (sampling the extreme line wings). The He I and He II lines were found to be too weak for such detailed investigation. In this fashion, a radial velocity was derived for each of the phase bins in the two seasons and these were fitted with a function of the form: $\gamma + K \cos 2\pi(\phi + \phi_0)$. The values of K, ϕ_0 and γ of these fits for the specified lines and values of a and σ can be found in Table 6.

The results in Table 6 can be summarized as follows: (i) there appear to be some variations in K and γ for the individual lines of the Balmer series but there are no consistent trends. Increasing a to 500 and 750 km s^{-1} (keeping $\sigma = 500$ km s^{-1}) made little difference to the values in Table 6; (ii) with the exception of the He II $\lambda\lambda$4541 and 4200 Å lines, there are no variations in ϕ_0 in Table 6; (iii) there is a rapid decline in the value of K from ~200 km s^{-1} at $a = 175$ km s^{-1} to ~120 km s^{-1} for all values of a from 500 km s^{-1} out to the extreme line wings at more than 1000 km s^{-1}; (iv) there are some peculiar results for the helium lines: although the K velocities for both He II λ4686 and He I $\lambda\lambda$4471 and 4921 Å are in reasonable accord with the Balmer results, the γ velocity is rather large and positive in both seasons. The γ

Table 6. Emission-line orbital variations.

	1988 March			1985 April		
	K (km s^{-1})	ϕ_0	γ (km s^{-1})	K (km s^{-1})	ϕ_0	γ (km s^{-1})
a=350						
σ=500						
Hβ	65 ±15	.33 ±.04	17 ±11	85 ±11	.23 ±.02	59 ± 8
Hγ	157 ±27	.23 ±.03	58 ±20	110 ±10	.25 ±.02	53 ± 7
Hδ	158 ±17	.26 ±.02	-2 ±11	121 ± 8	.22 ±.02	28 ± 6
Hε	122 ±20	.24 ±.03	0 ±14	171 ±11	.26 ±.01	11 ± 7
H8	196 ±26	.24 ±.03	95 ±18	143 ±20	.23 ±.02	84 ±14
HeII 4686	87 ±32	.25 ±.06	119 ±23	94 ±13	.21 ±.02	81 ± 9
HeII 4541& 4200	254 ±15	.46 ±.01	-192 ±11	151 ±32	.24 ±.03	-67 ±22
HeI 4471& 4921	177 ±36	.32 ±.03	147 ±25	95 ±38	.23 ±.06	156 ±27
All Balmer						
σ=175						
a=						
175	203 ± 9	.24 ±.01	29 ± 7	188 ±12	.25 ±.01	51 ± 9
350	167 ±12	.23 ±.01	39 ± 8	142 ± 5	.24 ±.01	51 ± 4
525	129 ± 8	.25 ±.01	29 ± 5	116 ± 3	.24 ±.01	49 ± 2
700	122 ±11	.26 ±.02	25 ± 8	109 ± 5	.24 ±.01	45 ± 4
875	134 ±13	.26 ±.02	23 ± 9	114 ±13	.24 ±.02	41 ± 9
1050	132 ±17	.27 ±.02	29 ±12	129 ±21	.24 ±.03	30 ±15

velocities for the He II $\lambda\lambda$4541 and 4200 Å lines are large and negative and the values of K and ϕ_0 for these lines in the 1988 March data are anomalous. Of course, the γ velocities can be distorted by weak, unresolved lines of other species.

The most important result from Table 6 is the decline in K from line centre to wings. This effect is consistent with the results of BFS (1984c), who noted that the spectroscopic variations in their data were clearer in the line peaks than in the line barycentres. The lack of variation of ϕ_0 with a in Table 6 indicates that the variation of the line peaks is in phase with the line wings. The effect is clearly visible as a 'V/R' variation in the phased spectra displayed in Fig. 5: the blue peak of the emission lines is enhanced near phase 0.25 and the red peak is enhanced near phase 0.75. In order to verify this conclusion in another way, we measured the V/R ratio by dividing each line about a central wavelength (given by the rest wavelength shifted according to the ephemerides in Table 5b), summing the flux to calculate the equivalent widths of the red and violet halves separately and taking the ratio of these values. This procedure removes the orbital motion as determined by the line wings and was carried out for the Balmer lines from Hβ up to H8 simultaneously. Restricting the summation to run from the central wavelength to only 300 km s^{-1} into the line wings resulted in a clear V/R variation whose amplitude, orbital phase of maximum and mean value are given in Table 7.

Table 7. Orbital variations of V/R.

	1988 March			1985 April		
Balmer	A	ϕ_{max}	mean	A	ϕ_{max}	mean
	0.19 ±.06	.33 ±.05	1.06 ±.04	0.13 ±.02	.26 ±.03	1.00 ±.01
He II 4686						
	0.62 ±.15	.28 ±.05	1.3 ±.1	0.32 ±.1	.37 ±.05	1.09 ±.08

Fig. 5 creates the impression that the effect is present in the He II λ4686 Å line; the numerical values in Table 7 confirm this. The V/R variation disappears in both the Balmer and He II λ4686 Å lines if the summation range extends to 1400 km s^{-1} from the central wavelength, i.e. the entire line profile. Also, there appear to be no variations in equivalent width (i.e. V + R) with orbital phase. There is weak evidence that the V/R variation is not quite in phase with the emission line wings, with maximum occurring later than 0.25.

We attempted to determine whether the narrow component responsible for the V/R variation could be seen as an 's-wave' in trailed spectra. To this end, the binned spectra were displayed as an image with orbital phase in one dimension, wavelength in the other and intensity proportional to the flux in the spectrum at that orbital phase and wavelength. The signal-to-noise ratio was not sufficient to distinguish the narrow component at all phases so no definite statement can be made. However, it should be noted that there is some evidence that there is repetitive 'fine structure' in the line profiles in Fig. 5. For example, the Hδ profiles in the top spectrum of each panel, which contains a prominent narrow component, is very similar in the two spectra. Some other line profiles in corresponding spectra in the two panels are also similar but the resolution and signal-to-noise ratio are not quite sufficient to be sure of the reality of the effect. We suggest that this structure, if real, is not simply due to the V/R variation discussed above but may be akin to the multiple components seen in the line profiles of polars such as V834 Cen (Rosen, Mason & Cordova 1987). Better resolution and signal-to-noise than available here will be required to confirm this suggestion.

4.4 MASSES

We now demonstrate that, if CP Pup is a disc system, it is yet another cataclysmic variable in which considerable doubt remains about the accuracy of the methods for estimating the masses of the components.

We begin by assuming that the motion of the emission line source is the same as that of the primary white dwarf and adopting 120 km s^{-1} as the K-velocity of the white dwarf: this value was derived from the cross-correlation radial velocities (Table 5a) and would be characteristic of the steepest parts of the line profile. We note that the value of K for the 1985 April and 1988 March data are consistent with each other and also consistent with the values of K for $a > 500$ km s^{-1} in the double Gaussian technique (Table 6). Although the adopted value is somewhat higher than the value of 92 ± 18 km s^{-1} reported by DSD, we have already remarked upon the considerably poorer quality of their velocities compared with those reported here.

We now assume that the secondary star follows the *empirical* period–secondary mass relationship (Patterson 1984), which in turn depends on the secondary filling its Roche lobe and obeying a mass–radius relationship for the lower main sequence. The empirical period–secondary mass relationship yields significantly lower masses than the theoretical relationship (e.g. Warner 1976); a discussion of these relationships and an attempt to justify use of the former can be found in Patterson (1984). The resulting secondary mass is 0.11 $M_\odot$ and this, together with the orbital period of 5300 s and adopted K, when inserted into the mass function, leads to a relationship between the orbital inclination and the white-dwarf mass which is labelled $M_2 = 0.11$ in Fig. 6.

Another constraint comes from assuming that the width of the emission lines result from Keplerian rotation in a disc surrounding the white dwarf (see Section 4.1). We have estimated the full width at zero intensity for the Balmer emission lines in both seasons and find a value of 2700 km s^{-1}. Assuming that the velocity of the extreme wings is the Keplerian velocity at the surface of the white dwarf yields the line labelled $V_{\rm Kep} = 1350$ in Fig. 6. The intersection of

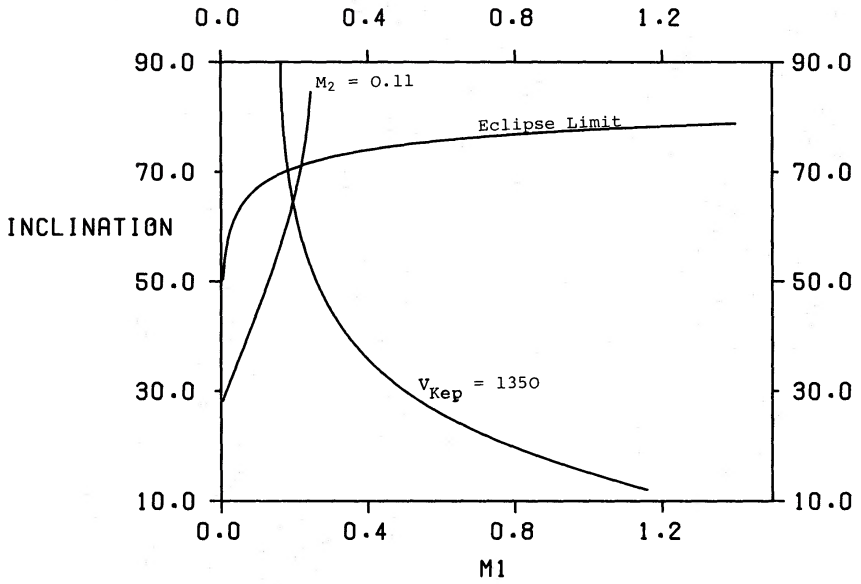

Figure 6. Plot of white-dwarf mass (in solar units) versus orbital inclination (in degrees) for the dynamical solution discussed in the text. The curve labelled $M_2 = 0.11$ is the mass function for a secondary mass of 0.11 $M_\odot$ together with the adopted K_1 of 120 km s^{-1}. The curve labelled $V_{\rm Kep} = 1350$ represents the inclination (in degrees) and white-dwarf mass (in $M_\odot$) required to yield a Keplerian velocity of 1350 km s^{-1} at its surface. The third curve results from the absence of deep eclipses in the light curve.

these lines occurs for large inclination angles. An upper limit to the inclination angle can be set by the absence of deep eclipses. The centre of the disc is eclipsed in the inclination is larger than the remaining line in Fig. 6.

Although a formal solution is available from Fig. 6, we are reluctant to put any reliance on it: the large inclination implied is incompatible with the value of about 30° found from analysing the motion of the ejecta (DSD) and the low amplitude of the ellipsoidal variations of the secondary (Szkody & Feinswog 1988). The mass of the white dwarf would also be extremely low (DSD) and in conflict with theoretical models of nova outbursts.

Almost no assumption made in the analysis just presented has escaped criticism. For instance, the assumption has been questioned that the secondary obeys the mass–radius relationship for the lower main sequence from which the period–secondary mass relationship is derived. Instead, it is proposed that the secondary is undermassive for its size as a consequence of the mass transfer process. For example, Wade & Horne (1988), using the mass ratio and inclination found from the analysis of the quiescent eclipses (Wood *et al.* 1986) and the *K*-velocity of the secondary derived from their infrared spectroscopy, find that the secondary in the dwarf nova Z Cha is substantially less massive than predicted by the theoretical period–secondary mass relationship (Warner 1976). The mass of the secondary in Z Cha is, however, compatible with the empirical period–secondary mass relationship of Patterson (1984). In the present case, reducing the mass of the secondary moves the mass function curve upwards thereby reducing the overlap with the linewidth constraint. The feasible region in Fig. 6 could be increased by reverting to the theoretical period–secondary mass relationship. It is interesting to note that the dwarf nova T Leo ($P_{\rm orb} = 85$ min, Shafter & Szkody 1984) has a shorter orbital period than CP Pup and shows an even larger *K* velocity in its emission lines (135 km s^{-1}). Had Shafter & Szkody (1984) applied the empirical (and not the theoretical) period–secondary mass relationship to T Leo they would have been unable to obtain a dynamical solution consistent with all their data.

The linewidth constraint in Fig. 6 is, of course, a lower limit so that arguing that the disc may not extend to the surface of the white dwarf reduces the feasible region and compounds the problem. If the linewidth is not entirely due to rotational Doppler broadening – Stark broadening being significant for example – the linewidth curve would be moved down in Fig. 6.

We believe, however, that the present problem (and the situation in regard to T Leo) originates in the anomalously large K found for the emission lines. The two most reliable dynamical models of Z Cha discussed by Wade & Horne (1988) ('P' and 'K' in their table 4) predict values of K of 56 and 64 km s^{-1} for the emission lines in that system; the observed value is 88 km s^{-1} (Marsh, Horne & Shipman 1987). The implication is that the emission lines do not share the motion of the white dwarf. The emission line anomalies seen in many cataclysmic variables and discussed in Section 3.3 support this view. Marsh *et al.* (1987) suggest that the accretion disc in Z Cha is distorted. Whether or not there exists an accretion disc in CP Pyp is not yet established; some discussion of this question will follow below.

5 Discussion

5.1 PHOTOMETRY

The mechanism for the photometric modulation is not obvious. However, it does not appear to be the canonical bright spot whose varying aspect is responsible for the orbital hump seen in systems such as Z Cha (Wood *et al.* 1986): the photometric modulation has variable amplitude and pulse shape, sometimes with a large duty cycle (e.g. run S4244), and is generally unlike the truncated cosine curve which approximates the shape of the orbital hump due to the bright spot.

As the orbital period of CP Pup is close to that of the SU UMa dwarf novae, Warner (1985) suggested that the photometric modulation might be a superhump such as are seen in all SU UMa stars during superoutburst. In this connection it is of interest to note that the period of superhumps is longer than the orbital period and decreases during a superoutburst; the shape of the superhump also changes.

Another possibility is that the photometric modulation is due to heating of the secondary, as has been suggested for V1500 Cyg (Patterson 1979; Stockman *et al.* 1988); we note, however, that the orbital phase (defining superior conjunction of the emission lines as phase 0, see Table 5b) at which the photometric maximum occurs in the 1988 March data is 0.04 ± 0.01, so the rear of the secondary is being presented to the observer at this time. Somewhat confusingly, photometric maximum does not always occur at the same orbital phase: in S3498, there are two well-defined maxima at HJD 6165.376 and 6165.438 (± 0.004) which occur at orbital phase 0.68 ± 0.07.

As remarked above, the light curve is at times similar to those of the polars, so the photometric modulation could be due to the varying visibility of an accretion column. If so, the lack of easily detectable circular polarization or a spectroscopic signature characteristic of the polars (see Section 5.2) implies that the column is more akin to those of the intermediate polars than the polars. The amplitude modulation and period differences in the photometric data were suggestive of the possibility of two closely-spaced photometric periods, perhaps the orbital period and the spin period of a slightly asynchronized magnetic white dwarf (analogous to Stockman, Schmidt & Lamb's model for V1500 Cyg). We may speculate that the observations of Warner (1985) would be accounted for by a relatively small contribution from the component at the orbital period; a larger contribution from this component would then account for the amplitude changes in the new data discussed here.

5.2 SPECTROSCOPY

Although the high excitation lines present in the spectrum of CP Pup are also seen in the polars, their orbital variation is not similar to the polars. Time-resolved spectroscopy of polars (e.g. Mukai 1988) is usually interpreted in terms of a broad component on which are superimposed one or more narrower components (V834 Cen being perhaps the most complex example: Rosen *et al.* 1987). With the exception of AM Her, which has shown a variable K velocity for the broad component down to 147 km s^{-1} (Crosa *et al.* 1981), the K velocity of the broad component exceeds 200 km s^{-1} and can be as high as 600 km s^{-1} (V834 Cen, Rosen *et al.* 1987). The K velocity of 120 km s^{-1} for the wings of the lines in CP Pup is modest by comparison. Although the spectral features seen in CP Pup are very similar to those seen in V1500 Cyg, the orbital variation of the lines is not (Kaluzny & Chlebowski 1988). Kaluzny & Chlebowski state that the spectrum of V1500 Cyg is like that of the polars with a narrow component superimposed on a broad base and they find a double wave variation with orbital phase in the broad component.

The high excitation lines seen in CP Pup are also seen in ex-novae; the possibility of doubling in the emission lines together with their orbital variation is more akin to cataclysmic variables, in which it is thought that there is a disc. For example, the similar phasing of the V/R variation and the velocity variations of the wings of the emission lines is similar to the behaviour seen in SW UMa (Shafter *et al.* 1986) in which the narrow component in the emission lines is almost in phase with the wings. We note in passing that it was the slight lag between the wings and the narrow component that led Shafter *et al.* (1986) to propose a region of enhanced emission on the edge of the disc diametrically opposite the bright spot; if the V/R variation slightly lags the wings in CP Pup (Table 7), a similar interpretation would place the region of enhanced emission on the edge of the disc about 120° downstream from the bright spot. Unlike CP Pup, the narrow component seen in the emission lines of T Leo is antiphased with the wings; if this component is due to a region of enhanced emission, this region appears to be located on the leading side of the disc, being closest to the observer at about orbital phase 0.15. No quadrant of the disc remains to be suggested for harbouring regions of enhanced emission!

The existence of a very fast nova outburst with mass ejection from a white dwarf of such low mass as inferred for CP Pup would present a puzzle for the theory of nova outbursts (Kovetz & Prialnik 1985; Sparks & Kutter 1987; Livio, Shankar & Truran 1988 and references therein). Note that the only way to avoid the conclusion that the white-dwarf mass in CP Pup is very low is either to *increase* the mass of the secondary substantially (by use of the theoretical period–secondary mass relationship, for example) or to propose that the K velocity of the white dwarf is much less than 120 km s^{-1}. If the emission lines in CP Pup are not formed in a disc, they would not be expected to share the motion of the white dwarf. However, as noted above, a dynamical solution for T Leo can be obtained only if the theoretical period–secondary mass relationship is used (Shafter & Szkody 1984). Even so, the resulting estimate of the mass of the white dwarf in that system is still very low (0.35–0.4 $M_{\odot}$). We believe that the weight of evidence in the literature has accumulated to the point where the use of emission-line radial velocity curves to measure the mass of the white dwarf in cataclysmic variables should be abandoned until the anomalies are understood.

6 Conclusion

We conclude that the nature of the old nova is yet to be established. It is of interest that Shafter & Szkody (1984) considered the possibility of a magnetic white dwarf in T Leo and estimated

that a magnetic field of less than 1 MG was required to phase-lock such a compact system. They also mentioned that no circular polarization would be observable if the magnetic field were so small. Warner & O'Donoghue (1987) have suggested that V2051 Oph harbours a white dwarf with a low magnetic field. The new data presented above have yielded no compelling evidence that CP Pup is a magnetic nova like V1500 Cyg; the most suggestive indirect evidence to emerge from this study is the behaviour of the photometric modulation. Clearly, an extensive photometric study of CP Pup is required.

Acknowledgments

We are grateful to I. McHardy for the *EXOSAT* observation and to D. Winget and C. Clemens for assistance in arranging the contemporaneous photometry at SAAO and Mt Stromlo. WW thanks A. C. Ilidio and ADG thanks P. Purnell-Grauer and L. Ferrario for assistance at the telescope. Allen Shafter and John Menzies discussed their radial velocity measuring techniques and generously made their programs available.

References

Becker, R. H. & Marshall, F. E., 1981. *Astrophys. J.*, **244,** L93.
Bianchini, A., Friedjung, M. & Sabbadin, F., 1985a. *Inf. Bull. Var. Stars No. 2650.*
Bianchini, A., Friedjung, M. & Sabbadin, F., 1985b. In: *Proceedings of the Frascati Workshop: Multifrequency Behaviour of Galactic Accreting Sources,* p. 82, ed. Giovanelli, F., Frascati.
Bianchini, A., Friedjung, M. & Sabbadin, F., 1985c. In: *Proceedings of the ESA Workshop: Recent Results On Cataclysmic Variables,* p. 77, ESA SP-236, Noordwijk.
Campbell, B., 1976. *Astrophys. J.*, **207,** L41.
Campolonghi, F., Gilmozzi, R., Guidoni, U., Messi, R., Natali, G. & Wells, J., 1980. *Astr. Astrophys.*, **85,** L4.
Cordova, F. A. & Mason, K. O., 1983. In: *Accretion-Driven Stellar X-Ray Sources,* p. 147, eds Lewin, W. H. G. & van den Heuvel, E. P. J., Cambridge University Press.
Cropper, M., 1986. *Mon. Not. R. astr. Soc.*, **222,** 225.
Crosa, L., Szkody, P., Stokes, G., Swank, J. & Wallerstein, G., 1981. *Astrophys. J.*, **247,** 984.
Deeming, T. J., 1975. *Astrophys. Space Sci.*, **36,** 137.
Duerbeck, H. W., Seitter, W. C. & Duemmler, R., 1987. *Mon. Not. R. astr. Soc.*, **229,** 653.
Glass, I. S., 1982. *SAAO Facilities Manual.*
Hessman, F. V., 1988. *Astr. Astrophys. Suppl.*, **72,** 515.
Hutchings, J. B. & McCall, M. L., 1977. *Astrophys. J.*, **217,** 775.
Kaitchuck, R. H., Honeycutt, R. K. & Schlegel, E. M., 1983. *Astrophys. J.*, **267,** 239.
Kaluzny, J. & Chlebowski, T., 1988. *Astrophys. J.*, **332,** 287.
Kaluzny, J. & Semeniuk, I., 1987. *Acta Astr.*, **37,** 349.
Kovetz, A. & Prialnik, D., 1985. *Astrophys. J.*, **291,** 812.
Kruszewski, A., Semeniuk, I. & Duerbeck, H. W., 1983. *Acta Astr.*, **33,** 339.
Lanning, H. H. & Semeniuk, I., 1981. *Acta Astr.*, **31,** 175.
Liebert, J. & Stockman, H. S., 1985. In: *Cataclysmic Variables and Low-Mass X-Ray Binaries,* p. 151, eds Patterson, J. & Lamb, D. Q., Reidel, Dordrecht, Holland.
Livio, M. & Shara, M. M., 1987. *Astrophys. J.*, **319,** 819.
Livio, M., Shankar, A. & Truran, J. W., 1988. *Astrophys. J.*, **330,** 264.
Loumos, G. L. & Deeming, T. J., 1978. *Astrophys. Space Sci.*, **56,** 285.
Marsh, T. R., Horne, K. & Shipman, H. L., 1987. *Mon. Not. R. astr. Soc.*, **225,** 551.
Mironov, A. V., Moshkalev, V. G. & Shugarov, S. Y., 1983. *Inf. Bull. Var. Stars No. 2438.*
Mukai, K., 1988. *Mon. Not. R. astr. Soc.*, **232,** 175.
Nather, R. E. & Warner, B., 1971. *Mon. Not. R. astr. Soc.*, **152,** 209.
Patterson, J., 1978. *Astrophys. J.*, **225,** 954.
Patterson, J., 1979. *Astrophys. J.*, **231,** 789.
Patterson, J., 1984. *Astrophys. J. Suppl.*, **54,** 443.
Piccioni, A., Guarnieri, A., Bartolini, C. & Giovanelli, F., 1984. *Acta Astr.*, **34,** 473.
Pringle, J. E., 1981. *Ann. Rev. Astr. Astrophys.*, **19,** 137.

Robinson, E. L., 1976. *Ann. Rev. Astr. Astrophys.*, **14,** 119.
Robinson, E. L., 1983. *Cataclysmic Variables and Related Objects, IAU Colloq. No. 72,* p. 1, eds Livio, M. & Shaviv, G., Reidel, Dordrecht, Holland.
Rosen, S. R., Mason, K. O. & Cordova, F. A., 1987. *Mon. Not. R. astr. Soc.,* **224,** 987.
Schlegel, E. M., Honeycutt, R. K. & Kaitchuck, R. H., 1983. *Astrophys. J. Suppl.,* **53,** 397.
Schneider, D. P. & Young, P., 1980. *Astrophys. J.,* **238,** 946.
Shafter, A. W., 1983. *Astrophys. J.,* **267,** 222.
Shafter, A. W. & Szkody, P., 1984. *Astrophys. J.,* **276,** 305.
Shafter, A. W., Szkody, P. & Thorstensen, J. R., 1986. *Astrophys. J.,* **308,** 765.
Shafter, A. W., Robinson, E. L., Crampton, D. & Warner, B., 1987. *Bull. Am. astr. Ass.,* **19,** 1058.
Sparks, W. M. & Kutter, G. S., 1987. *Astrophys. J.,* **321,** 394.
Stockman, H. S., Schmidt, G. D. & Lamb, D. Q., 1988. *Astrophys. J.,* **332,** 282.
Szkody, P. & Brownlee, D. E., 1977. *Astrophys. J.,* **212,** L113.
Szkody, P. & Feinswog, L., 1988. *Astrophys. J.,* **334,** 422.
Thorstensen, J. R., 1986. *Astr. J.,* **91,** 940.
Tonry, J. & Davis, M., 1979. *Astr. J.,* **84,** 1511.
Wade, R. & Horne, K., 1988. *Astrophys. J.,* **324,** 411.
Warner, B., 1976. *Structure and Evolution of Close Binary Systems, IAU Symp. No. 73,* p. 85, eds Eggleton, P. P., Mitton, S. & Whelan, J. A. J., Reidel, Dordrecht, Holland.
Warner, B., 1985. *Mon. Not. R. astr. Soc.,* **217,** 1P
Warner, B. & O'Donoghue, D., 1987. *Mon. Not. R. astr. Soc.,* **224,** 733.
Watts, D. J., Bailey, J., Hill, P. W., Greenhill, J. G., McCowage, C. & Carty, T., 1986. *Astr. Astrophys.,* **154,** 197.
Wood, J., Horne, K., Berriman, G., Wade, R., O'Donoghue, D. & Warner, B., 1986. *Mon. Not. R. astr. Soc.,* **219,** 629.
Young, P., Schneider, D. P. & Schectman, S. A., 1981. *Astrophys. J.,* **244,** 259.